

## DEVELOPMENT AND DISEASE

# Elevated SMAD1/ $\beta$ -catenin molecular complexes and renal medullary cystic dysplasia in ALK3 transgenic mice

Ming Chang Hu<sup>1</sup>, Tino D. Piscione<sup>1,2</sup> and Norman D. Rosenblum<sup>1,2,\*</sup>

<sup>1</sup>Program in Developmental Biology, Research Institute, The Hospital for Sick Children, 555 University Avenue, Toronto, Ontario M5G 1X8, Canada

<sup>2</sup>Division of Nephrology, Department of Paediatrics, University of Toronto, 555 University Avenue, Toronto, Ontario M5G 1X8, Canada

\*Author for correspondence (e-mail: norman.rosenblum@sickkids.ca)

Accepted 13 March 2003

## SUMMARY

Renal dysplasia, the most frequent cause of childhood renal failure in humans, arises from perturbations in a complex series of morphogenetic events during embryonic renal development. The molecular pathogenesis of renal dysplasia is largely undefined. While investigating the role of a BMP-dependent pathway that inhibits branching morphogenesis in vitro, we generated a novel model of renal dysplasia in a transgenic (Tg) model of ALK3-receptor signaling. We report the renal phenotype, and our discovery of molecular interactions between effectors in the BMP and WNT signaling pathways in dysplastic kidney tissue. Expression of the constitutively active ALK3 receptor ALK3<sup>QD</sup>, in two independent transgenic lines caused renal aplasia/severe dysgenesis in 1.5% and 8.4% of hemizygous and homozygous Tg mice, respectively, and renal medullary cystic dysplasia in 49% and 74% of hemizygous and homozygous Tg mice, respectively. The dysplastic phenotype, which included a decreased number of medullary collecting ducts, increased medullary mesenchyme, collecting duct cysts and decreased cortical

thickness, was apparent by E18.5. We investigated the pathogenesis of dysplasia in these mice, and demonstrated a 30% decrease in branching morphogenesis at E13.5 before the appearance of histopathological features of dysplasia, and the formation of  $\beta$ -catenin/SMAD1/SMAD4 molecular complexes in dysplastic renal tissue. Increased transcriptional activity of a  $\beta$ -catenin reporter gene in ALK3<sup>QD</sup>;Tcf-gal mice demonstrated functional cooperativity between the ALK3 and  $\beta$ -catenin-dependent signaling pathways in kidney tissue. Together with our results in the dysplastic mouse kidney, our findings that phospho-SMAD1 and  $\beta$ -catenin are overexpressed in human fetal dysplastic renal tissue suggest that dysregulation of these signaling effectors is pathogenic in human renal dysplasia. Our work provides novel insights into the role that crucial developmental signaling pathways may play during the genesis of malformed renal tissue elements.

Key words: Renal dysplasia, ALK3, SMAD1,  $\beta$ -catenin, Signaling

## INTRODUCTION

Renal dysplasia, a polymorphic entity defined at the level of histopathology as malformation of renal tissue elements, is the leading cause of renal failure in children (Neu et al., 2002). Definition of the pathogenesis of renal dysplasia has been limited by a sporadic mode of inheritance, the small size of affected kindreds and the relative inaccessibility of dysplastic renal tissue in humans (Piscione and Rosenblum, 1999). However, identification of the molecules that control normal kidney development is beginning to provide insight into underlying pathogenic mechanisms (Pohl et al., 2002).

Normal kidney development is dependent on inductive interactions between the metanephric blastema, a mesenchymal tissue and the ureteric bud, an epithelial structure (reviewed by Saxen, 1987). Under the control of signals secreted by the metanephric blastema, the ureteric bud grows

as a lateral extension of the Wolffian Duct, and invades the metanephric blastema at 5 weeks gestation in the human and E10.5 in the mouse. Cells of the metanephric blastema adjacent to the tip of the ureteric bud are induced by the ureteric bud to undergo a mesenchymal-epithelial transformation. In reciprocal fashion, the metanephric blastema signals the ureteric bud to grow and branch, a process termed branching morphogenesis. Ongoing reciprocal inductive tissue interactions result in the formation of proximal epithelial nephron segments (glomerulus, proximal and distal tubules, loop of Henle) from blastemal progenitors, and cortical and medullary collecting ducts, the terminal components of the nephron, from the ureteric bud. Beginning at E15.5–E16.5, the murine kidney becomes further patterned into an outer cortex (comprising glomeruli, proximal and distal tubules, and cortical collecting ducts), and an inner medulla composed of Henle's loop (a blastema-derived structure) and medullary

collecting ducts. During the final stages of development in utero, the first five branches of the ureteric bud undergo transformation into the pelvis and calyces.

Human renal malformations are typically classified as aplasia, hypoplasia or dysplasia. Renal hypoplasia is defined as a reduction in the number of normally formed nephrons. Since each ureteric bud branch induces a discrete subset of blastemal cells to form a nephron, it is hypothesized that ureteric bud branching is proportional to the final number of nephrons that are formed. Consistent with this concept, diminution of ureteric bud branching is thought to represent one pathogenic pathway during the genesis of renal hypoplasia. By contrast, renal dysplasia is characterized by variable degrees of tissue malformation in the renal cortex, medulla or both (reviewed by Bernstein, 1992). In its most extreme form, the dysplastic kidney either fails to form (renal aplasia) or consists of undifferentiated blastema associated with primitive ureteric bud branches with or without cystic transformation, the so-called multicystic dysplastic kidney. Less severe forms of dysplasia are characterized by discrete foci of malformed tissue elements, or dysplasia limited to the peripheral cortex and medulla, or restricted to the medulla, alone. Each of these forms has been associated with a variety of clinical entities, including lower urinary tract obstruction and multi-organ malformation syndromes.

Mutations in genes encoding a variety of molecules, including transcription factors, growth factors, growth factor receptors and heparan sulfate proteoglycans, cause renal dysplasia (reviewed by Piscione and Rosenblum, 1999). Among these crucially important gene products are members of the bone morphogenetic protein (BMP) family of secreted growth factors. Several members of the BMP family are expressed in overlapping but distinct domains during murine kidney development. The spatial and temporal expression of BMP2, and its cell-surface receptor, activin-like kinase 3 (ALK3; BMPRI1A – Human Gene Nomenclature Database), suggests a role for this secreted growth factor and receptor during mesenchymal-epithelial interactions in the embryonic kidney (Dewulf et al., 1995; Dudley and Robertson, 1997; Flanders et al., 2001). The early embryonic lethality observed in *Bmp2*<sup>-/-</sup> and *Alk3*<sup>-/-</sup> mice (Mishina et al., 1995; Tremblay et al., 2001; Zhang and Bradley, 1996) precluded analysis of their respective roles during renal development. However, our studies in *in vitro* models of branching morphogenesis have defined an inhibitory role for the BMP2/ALK3 signaling through the cytoplasmic effector SMAD1 (MADH1 – Human Gene Nomenclature Database). BMP2 inhibits ureteric bud branching in embryonic kidney explants and is bound to the surface of collecting duct cells by ALK3 (Piscione et al., 1997). Interruption of ALK3 in an *in vitro* model of collecting tubule formation abrogates the inhibitory functions of BMP2 and constitutive signaling of an activated form of ALK3 is inhibitory (Gupta et al., 2000; Piscione et al., 2001). Collectively, these observations suggest that the ALK3 can function downstream of ligands such as BMP2 to inhibit branching morphogenesis *in vivo*.

To gain insight into the functions of the ALK3 pathway *in vivo*, we generated transgenic mice expressing a constitutive active form of ALK3 in the ureteric bud lineage and observed a novel medullary cystic dysplastic phenotype. We investigated the pathogenesis of this phenotype and demonstrated decreased branching morphogenesis during early embryonic renal

development, which is consistent with our previous findings *in vitro*. However, in contrast to our prediction that decreased branching morphogenesis would lead to renal hypoplasia, we observed renal medullary cystic dysplasia with increased penetrance in homozygous transgenic mice. In experiments to identify mechanisms by which ALK3 signaling could generate this phenotype, we observed: increased  $\beta$ -catenin expression in affected mice; increased expression of a TCF transcriptional reporter in compound transgenic progeny of *Tcf-gal* and *TgALK3<sup>QD/QD</sup>* mice; and molecular complexes consisting of  $\beta$ -catenin and SMAD1, an ALK3 effector, in kidney tissue from transgenic mice. Our finding that SMAD1 and  $\beta$ -catenin are overexpressed in dysplastic human kidney tissue suggests that dysregulation of BMP and WNT signaling effectors is pathogenic in human renal dysplasia.

## MATERIALS AND METHODS

### Generation of *ALK3<sup>QD</sup>* transgenic mice

A 1.7 kb *BglIII-BamHI* fragment containing a hemagglutinin (HA)-tagged human *ALK3<sup>QD</sup>* cDNA, consisting of an aspartic acid to glutamine mutation at position 233 (Hoodless et al., 1996) (kindly provided by Dr L. Attisano), was subcloned into pBS/*Hoxb.7-linker-h $\beta$ glo3'* (Srinivas et al., 1999a) (a generous gift of Dr F. Costantini), excised from the vector with *PmeI* and injected into pronuclei of CD1 mouse zygotes. Transgenic founders were identified by Southern blot of mouse tail genomic DNA, using a 915 bp *BamHI-EcoRI* fragment of the transgene spanning part of the 3' human  $\beta$ -globin untranslated region. Germline transmission of the transgene was determined by breeding founder mice with non-transgenic CD1 mice. Homozygote transgenic mice were generated by interbreeding hemizygotes. Hemizygous and homozygous transgenic mice were distinguished by comparing the intensity of individual bands of genomic DNA on Southern blots.

### Antibodies and tissue

For immunohistochemistry, the following antibodies were used: anti-HA (1:10 dilution; Roche Molecular Biochemicals-Boehringer Mannheim, Laval, P.Q.); anti- $\beta$ -catenin (1:25 dilution; Upstate Biotech, Lake Placid, NY); anti-E-cadherin (1:25 dilution; Santa Cruz Biotechnology, CA); and anti-phospho-SMAD1 (1:10; Cell Signaling Tech, Beverly, MA). For western analysis, these primary antibodies were diluted 1:500 as were antibodies for MYC (Santa Cruz, CA), HA (Amersham Pharmacia Biotech, Piscataway, NJ) and SMAD1 (Upstate Biotech, Lake Placid, NY). Chemiluminescence was performed using commercially available reagents (ECL kit; Amersham Pharmacia Biotech, Piscataway, NJ). Human kidney tissue was kindly provided by Dr G. Ryan with the approval of the Research Ethics Boards at Mount Sinai Hospital, Toronto and The Hospital for Sick Children, Toronto.

### Immunohistochemistry

Paraffin wax-embedded sections (4  $\mu$ m) of adult or embryonic kidney tissue were pre-treated by microwave heating in 0.01 M citrate buffer (pH 6.0) in a microwave pressure cooker for 14 minutes, including a boiling period of 1.5 minutes. After a 10 minute incubation in 1% H<sub>2</sub>O<sub>2</sub> to quench endogenous peroxidase activity, tissue sections were incubated with primary antibody, followed by ABC complex, and then developed with peroxidase substrate AEC (Zymed Laboratories, San Francisco, CA). Ureteric bud-derived structures were identified with Dolichos Biflorus Agglutinin (DBA; Vector Labs, Burlington, ON). Slides were imaged by brightfield and immunofluorescence microscopy. Human tissues incubated with anti-phospho-SMAD1 antibody were treated with 0.01% pepsin in 10 mM HCl for 30-45

minutes at 37°C after treatment with H<sub>2</sub>O<sub>2</sub> and prior to incubation with antibodies.

### Analysis of ureteric bud branching in embryonic kidneys

Kidneys were surgically dissected from embryonic (E) day 13.5 pregnant mice and cultured as described previously (Piscione et al., 1997). Ureteric bud-derived structures were identified in whole-mount kidney specimens with fluorescein isothiocyanate (FITC)-conjugated DBA (20  $\mu$ g/ml; Vector Labs, Burlington, ON) as described. Ureteric bud branch points were defined as the intersection between two connected branches (Grisaru et al., 2001).

### In situ cell proliferation assay

Ureteric bud cell proliferation in embryonic kidney was assayed with 5-bromo-2'-deoxyuridine, as described previously (Cano-Gauci et al., 1999). Ureteric bud cell proliferation was calculated as the number of BrdU-labeled cells within the population of ureteric bud/collecting duct cells identified by DBA. Cell proliferation in postnatal mouse kidney was assayed by immunohistochemistry using anti-Ki-67 antibody (1:10 dilution; Roche Molecular Biochemicals-Boehringer Mannheim, Laval, P.Q.). The number of positive cells and the number of tubule cross-sections were counted in ten randomly selected areas imaged at 400 $\times$  magnification.

### TCF-reporter activity in kidney tissue

TCF-reporter activity was assayed in *Tcf-gal* mice, kindly provided by Dr B. Alman (Cheon et al., 2002). *Tcf-gal* mice express the *lacZ* gene downstream of a FOS minimal promoter and three consensus TCF-binding motifs.  $\beta$ -Galactosidase activity was assayed using published methods (Godin et al., 1998).

### Co-immunoprecipitation assay

Cell or tissue lysates were subjected to immunoprecipitation with anti-SMAD1 or anti- $\beta$ -catenin antibody, followed by adsorption to protein G plus-agarose (IP04; Oncogene, Boston, MA). Immunoprecipitated proteins were washed, separated by SDS-polyacrylamide gel electrophoresis and transferred to PVDF membrane.

### RT-PCR assay

First-strand cDNA was synthesized using total RNA as a template. PCR was then performed using the following primers encoding highly conserved regions within WNT11, WNT4, WNT2B, WNT5B, WNT7B and WNT6: sense, 5'-GAGTGCAAGTGTCACGGGGT-3'; and antisense, 5'-CAGCACCAGTGGAACTTGCA-3'. Thirty cycles of PCR amplification were performed using the following protocol: 30 cycles of 92°C for 1 minute, 59°C for 1 minute and 72°C for 1 minute.

### Data analysis

The pixel density of protein bands identified by immunoblotting was adjusted for the density of a control protein (i.e. actin, SMAD1 or  $\beta$ -catenin) in that sample. The adjusted values of protein were analyzed using the Stat-View statistical analysis program (version 4.01; Abacus

Concepts, Berkeley, CA). Mean differences were examined by Student's *t*-test (two-tailed) or by ANOVA. Significance was taken at a value of  $P < 0.05$ .

## RESULTS

### Transgenic mice expressing a constitutive active form of ALK3

Knockout mice have not been informative regarding the role of *Alk3* during renal development because homozygous-null mice die during gastrulation and heterozygote mice do not exhibit a phenotype (Mishina et al., 1995). We devised an alternative strategy in which we expressed a constitutive active HA-tagged *ALK3* allele, *ALK3<sup>QD</sup>*, downstream of a *Hoxb7* promoter element that restricts expression largely to the ureteric bud lineage (Kress et al., 1990) (Fig. 1A). We generated two lines of transgenic mice derived from two independent founders. We generated hemizygous (*TgALK3<sup>QD</sup>*) and homozygous (*TgALK3<sup>QD/QD</sup>*) transgenic progeny from each of the two founder transgenic mice (Table 1). In so doing, we observed that both hemizygous and homozygous Tg mice were fertile, and generated litters similar in size to those observed with control CD1 mice. The renal phenotypes observed in both lines were identical, which suggests that these phenotypes are directly referable to the expression of the transgene.

To demonstrate expression of the *ALK3<sup>QD</sup>-HA* transgene, we detected *ALK3<sup>QD</sup>-HA* protein in renal tissue by western analysis and immunohistochemistry using an anti-HA antibody (Fig. 1B,C). We detected the HA epitope in kidney tissue lysates from both hemizygous Tg and homozygous Tg mice (Fig. 1B). However, greater amounts were detected in homozygous mice, which is consistent with the increased gene dosage in these mice. Next, we studied the spatial expression of *ALK3<sup>QD</sup>-HA* in renal tissue sections. In hemizygous Tg mice, the HA epitope was detected in cortical collecting ducts and in medullary collecting ducts (Fig. 1C). The level of expression in these tubules was greatly increased in homozygous mice, which is consistent with the quantities identified in tissue lysates. Taken together, these results demonstrate that expression of the *ALK3<sup>QD</sup>* transgene was restricted to renal collecting ducts.

### Constitutive expression of activated ALK3 causes postnatal mortality associated with renal aplasia/dysplasia and renal medullary cystic dysplasia

To analyze the viability and renal developmental status of *ALK3<sup>QD</sup>* Tg mice, we examined litter size and viability, and

**Table 1. Incidence of renal phenotypes in *TgALK3* mice**

Transgenic group	Medullary cystic dysplasia* <i>n</i> (% total)	Aplasia/Dysgenesis† <i>n</i> (% total)	No defect <i>n</i> (% total)
<b>Line 1: <i>n</i>=161</b> ( <i>TgALK3<sup>QD</sup></i> and <i>TgALK3<sup>QD/QD</sup></i> )			
<i>TgALK3<sup>QD</sup></i> ( <i>n</i> =55)	106 (66)	10 (6)	45 (28)
<i>TgALK3<sup>QD/QD</sup></i> ( <i>n</i> =106)	28 (51)	1 (2)	26 (47)
	78 (74)	9 (8)	19 (18)
<b>Line 2: <i>n</i>=24</b> ( <i>TgALK3<sup>QD</sup></i> and <i>TgALK3<sup>QD/QD</sup></i> )			
<i>TgALK3<sup>QD</sup></i> ( <i>n</i> =14)	14 (58)	0 (0)	10 (71)
<i>TgALK3<sup>QD/QD</sup></i> ( <i>n</i> =10)	6 (43)	0 (0)	8 (57)
	8 (80)	0 (0)	2 (20)

\*28/106 mice in Line 1 and 3/14 mice in Line 2 demonstrated growth retardation and died by 2 months of age. All were homozygous Tg.

†In Line 1, 7/10 mice died within several days of birth. All were homozygous Tg and demonstrated bilateral renal aplasia or bilateral aplasia/dysgenesis. 3/10 failed to thrive and died by 1 month of age.

performed a gross anatomic analysis of the kidney (Table 1). Seven out of 161 (4.3%) mice in Tg Line 1 died within several days of birth. Postmortem examination revealed bilateral renal

aplasia in one mouse, and bilateral renal malformations consisting of a combination of aplasia and severe dysgenesis in six other mice. Southern analysis of genomic DNA revealed that these seven affected mice were homozygous Tg. All mice in Line 2 survived beyond the neonatal period. Thirty-four mice (31 in Line 1 and three in Line 2) demonstrated severe growth retardation and died between one and two months of age. All affected mice were homozygous Tg. Three of these mice were observed to have bilateral aplasia/dysgenesis. Histological examination in the remaining 31 showed medullary cystic dysplasia of variable severity (see below). Mice that survived beyond two months of age ( $n=144$ ) demonstrated no obvious abnormalities up to at least 7 months of age, by which time all were sacrificed. However, histological analysis revealed medullary cystic dysplasia in 89 of these mice. Thus, we observed renal aplasia/dysgenesis or medullary cystic dysplasia in 5% (10/185) and 65% (120/185) of Tg mice, respectively.

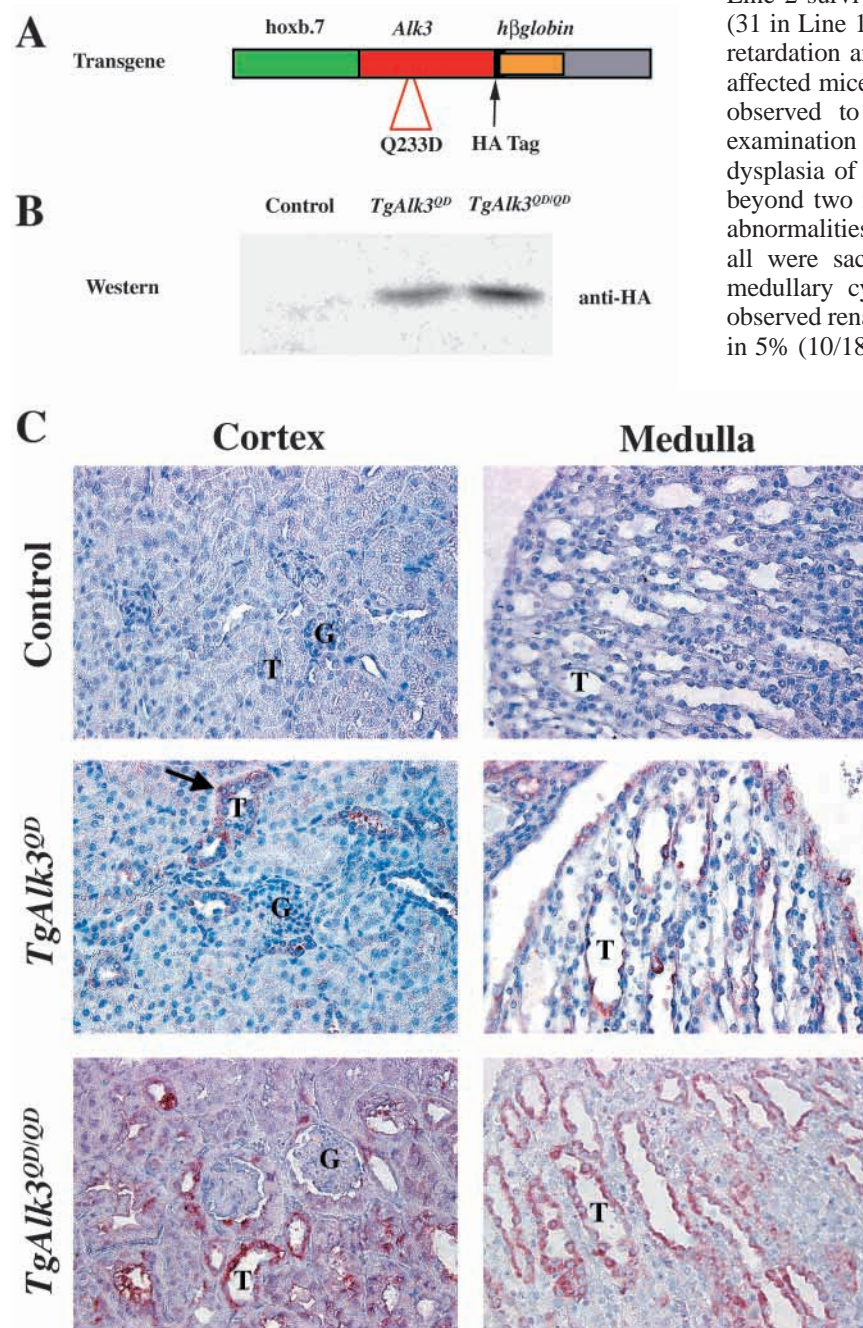
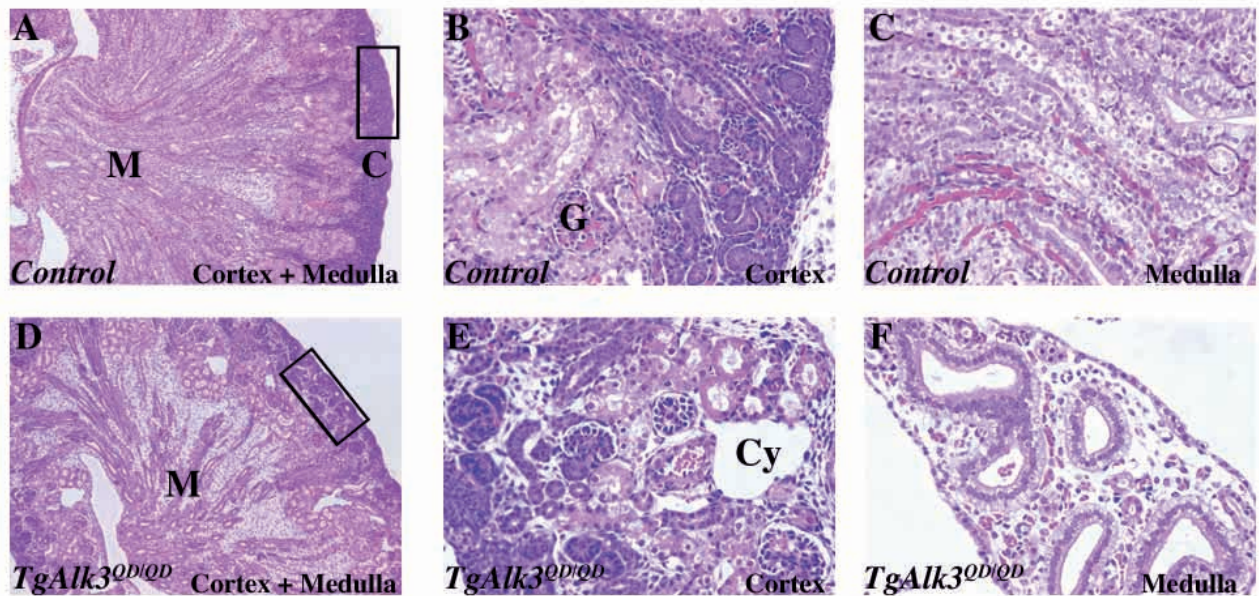


**Fig. 1.** Transgenic mice overexpressing ALK3<sup>QD</sup>. (A) Structure of the transgene. The positions of the *Hoxb7* promoter, Q233D mutation, the HA tag, and the human  $\beta$ -globin sequence are shown. (B) Western blot analysis of proteins isolated from mouse kidney at P10 showing expression of HA-tagged ALK3 in TgALK3<sup>QD</sup> mice and a marked increase in ALK3-HA levels in TgALK3<sup>QD/QD</sup> mice. (C) ALK3<sup>QD</sup>-HA expression in TgALK3<sup>QD</sup> mice at P10. Expression of the HA epitope was detected by immunohistochemistry using an anti-HA antibody (brown stain). HA was undetectable in the cortex and medulla of control kidneys. In hemizygous (TgALK3<sup>QD</sup>) mice, low levels of HA (arrow) were detected in cortical collecting ducts (T) and in medullary collecting ducts but not in glomeruli (G). In homozygous (TgALK3<sup>QD/QD</sup>) mice, much higher levels of HA were detected in a small subset of cortical tubules (T) and in medullary collecting ducts (T).

To identify the dysplastic renal phenotype in embryos and postnatal mice, we performed a histopathological analysis (Fig. 2). By E18.5, the crucial events during epithelial morphogenesis and patterning have occurred in the kidney. Homozygote Tg mice demonstrated marked abnormalities compared with control mice. The diameter of the outer cortex was decreased (compare boxed area in Fig. 2D with Fig. 2A, and Fig. 2E with Fig. 2B). The outer cortex is the site at which glomerular progenitors, termed comma and S-shaped bodies, form. Although these progenitors appeared normal qualitatively, the decreased number of elements suggested a primary or secondary defect in the number of inductive events. The medulla in TgALK3<sup>QD</sup> mice was remarkable because of a marked reduction in the number of medullary tubules (compare Fig. 2D,F with Fig. 2A,C), and an increase in interstitial matrix (Fig. 2D,F). These changes were accompanied by the formation of epithelial cysts in the inner and outer regions of the medulla and in the cortex (Fig. 2D,E). These histological abnormalities were also observed in heterozygous Tg mice, although the phenotype was observed in a minority of mice and was less severe (data not shown). At P10, the dysplastic phenotype could be readily identified in hemizygous Tg mice (Fig. 2H), and was more severe in homozygous Tg mice (Fig. 2I,J). In contrast to control mice (Fig. 2G), 50% of hemizygous Tg mouse kidneys were characterized by a decreased number of tubules in the medulla, increased intervening extracellular matrix, underdevelopment of the papilla, and the formation of cortical and medullary cysts (Fig. 2H). Abnormalities of a greater severity were observed in 74% of homozygous Tg mice (Fig. 2I,J). In these mice, the medulla was occupied by large cysts and extracellular matrix, and the cortex

## E18.5



## P10

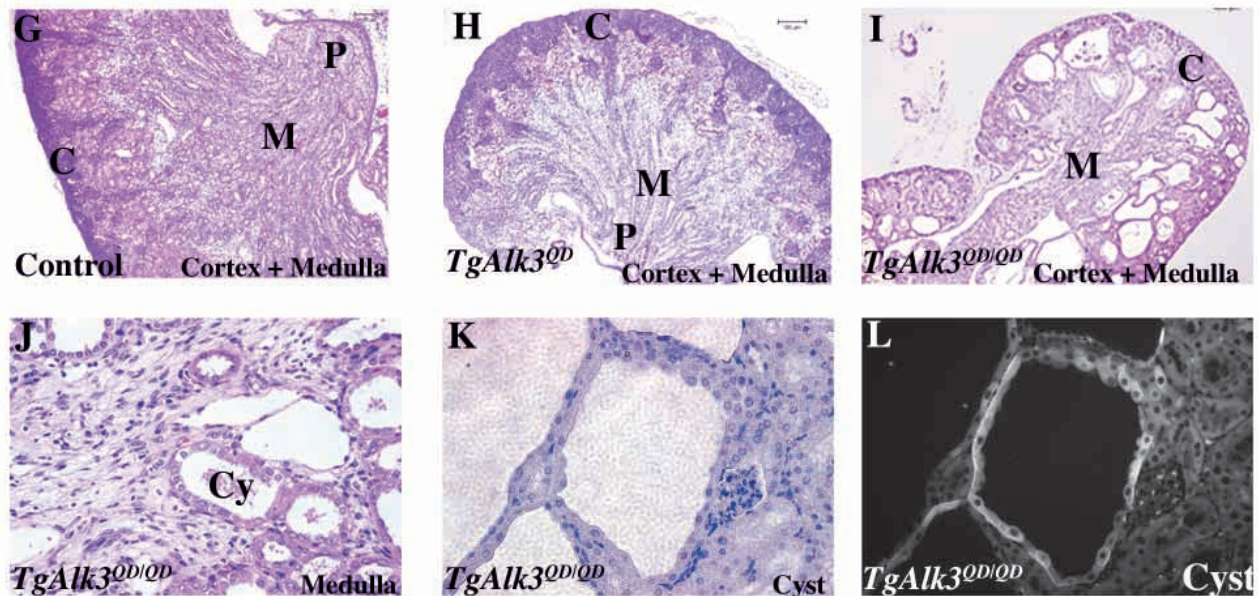


**Fig. 2.** Renal phenotype of *TgALK3<sup>QD</sup>* and *TgALK3<sup>QD/QD</sup>* mice at E18.5 (A-F) and P10 (G-L) in representative 4  $\mu$ m tissue sections. Sections in A-J are stained with Haematoxylin and Eosin. (A-F) E18.5. (A) The kidney of control mice is characterized by a well-differentiated cortex (C) and medulla (M). The box highlights the outer cortex. (B) Higher magnification view of the cortex in a control kidney. It is characterized by glomerular progenitors in the outer cortex and a mature glomerulus (G) in the deep cortex. (C) Higher magnification view of the medulla in a control kidney. It consists of a densely packed linear array of tubules. Note the lack of intervening mesenchyme. (D) The kidney of *TgALK3<sup>QD/QD</sup>* mice is characterized by decreased density of immature glomeruli in the outer cortex, cortical cysts, a paucity of medullary collecting ducts in the medulla, a marked increase in mesenchyme in the medulla and medullary cysts. (E) Higher magnification view of the kidney cortex of a *TgALK3<sup>QD/QD</sup>* mouse. Note the decreased density of glomerular progenitors in the outer cortex (compared with B) and the presence of a cyst (Cy). (F) Higher magnification view of the kidney medulla of a *TgALK3<sup>QD/QD</sup>* mouse. Note the cystic dilatation of tubules, the decreased density of tubules and the increase in intervening mesenchyme. (G-L) P10. (G) The kidney of a control mouse is characterized by a well-developed cortex, medulla and papilla (P). (H) The kidney of a *TgALK3<sup>QD</sup>* mouse is smaller in area. It exhibits fewer medullary tubules, has cysts in the cortex and medulla and has a smaller papilla. (I) The kidney of a *TgALK3<sup>QD/QD</sup>* mouse is malformed by large cysts in the cortex and medulla. The outer cortex is compressed. The medulla contains few tubules and shows a large increase in intervening mesenchyme. (J) Higher power view of the renal medulla of a *TgALK3<sup>QD/QD</sup>* mouse. Note the cystic tubules. Some are characterized by a cuboidal epithelium (Cy), whereas others have a squamous epithelium. The intertubular mesenchyme is increased and contains fibroblastic cells. (K,L) A medullary cyst in the kidney of a *TgALK3<sup>QD/QD</sup>* mouse stained with DBA. (L) Positive staining indicates that the cyst epithelium is of ureteric bud origin.

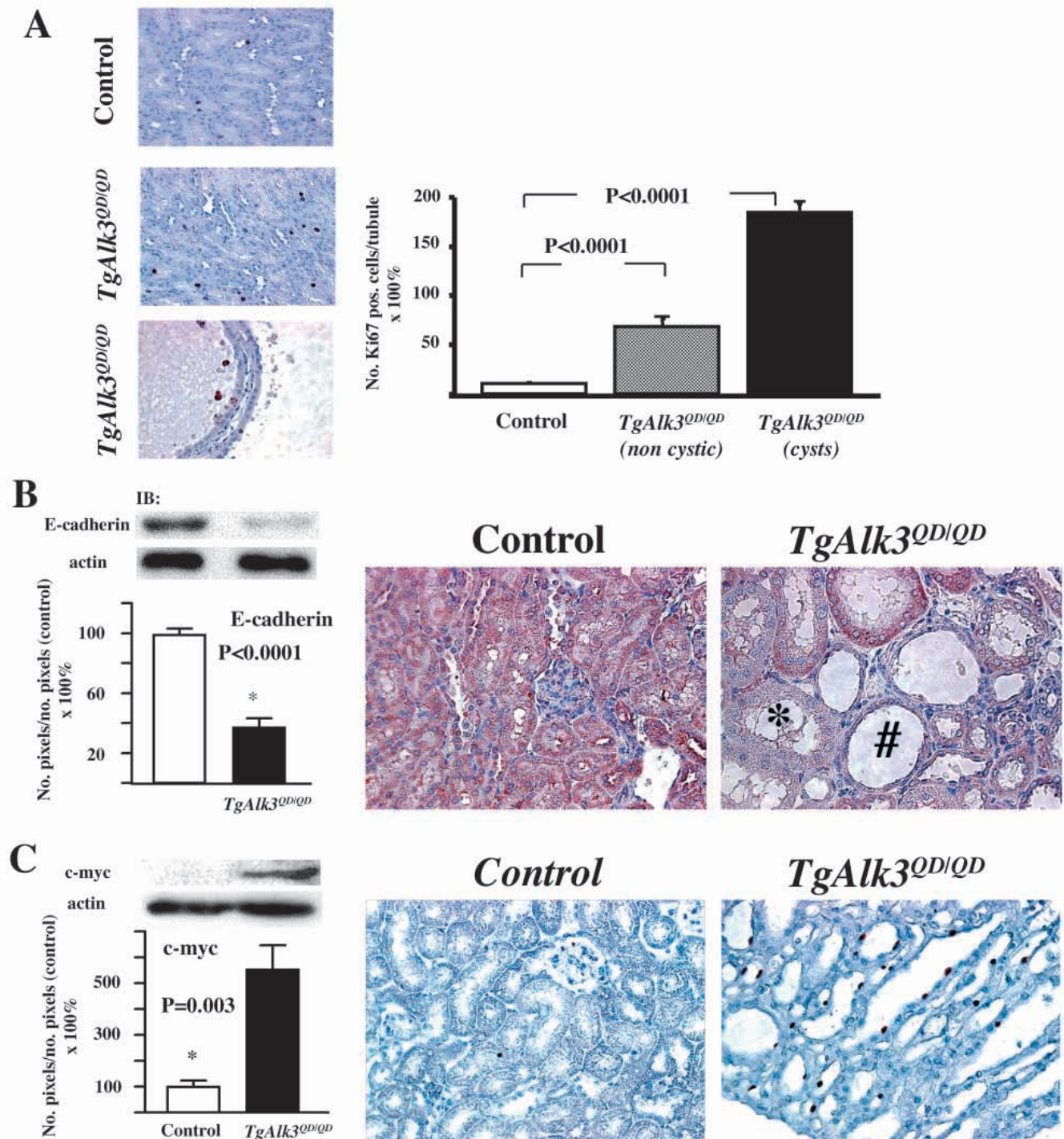


**Fig. 3.** Cellular changes in the kidneys of *TgALK3<sup>QD/QD</sup>* mice. (A) Cell proliferation in kidney tissue of P10 mice detected by anti-Ki67 and HRP-conjugated secondary antibodies. Left: Hematoxylin-stained tissue demonstrates a marked increase in the number of cells expressing Ki-67 (red) in non-cystic and cystic tissue elements of Tg mouse kidneys compared with control kidneys. Right: quantitation of cell proliferation showed a 6.4-fold and 17.1-fold increase in non-cystic and cystic tissue elements, respectively, of *TgALK3<sup>QD/QD</sup>* versus control mice. (B) E-cadherin expression is decreased in *TgALK3<sup>QD/QD</sup>* kidney tissue. Left: quantitation of E-cadherin protein in whole kidney lysate demonstrated a 64% decrease in *TgALK3<sup>QD/QD</sup>* versus control mice. Right: immunohistochemistry using anti-E-cadherin and HRP-conjugated secondary antibodies. E-cadherin is expressed in all epithelial tubules in control kidneys. By contrast, in *TgALK3<sup>QD/QD</sup>* kidney tissue, expression is reduced in a subset of tubules with cuboidal (\*) or squamous (#) epithelium. (C) MYC expression is increased in *TgALK3<sup>QD/QD</sup>* kidney tissue. Left: quantitation of MYC protein in whole kidney lysate demonstrated a 542% increase in *TgALK3<sup>QD/QD</sup>* versus control mice. Right: immunohistochemistry using anti-MYC and HRP-conjugated secondary antibodies. MYC is almost undetectable in control kidneys. By contrast, in *TgALK3<sup>QD/QD</sup>* kidney tissue, expression is markedly increased in cystic epithelium (red color marking cell nuclei). Data are mean $\pm$ s.d. Number of independent experiments were: E-cadherin,  $n=4$ ; MYC,  $n=6$ .

was reduced to a thin layer, perhaps as a result of compression caused by cysts. Analysis of cyst epithelium with DBA revealed positive staining, which suggests that ALK3-HA expressing cysts are derived from the ureteric bud lineage (Fig. 2K,L). Taken together, these findings suggest a pathological diagnosis of medullary cystic dysplasia with cortical cyst formation.

The dysplastic kidney is characterized by renal epithelial cell de-differentiation. Markers of de-differentiating epithelium include: transformation from a columnar or cuboidal to a squamous morphology; dysregulation of the cell cycle; loss of expression of epithelial-specific markers; and formation of epithelial cysts (Winyard et al., 1996). Demonstration of these abnormalities in kidney tissue helps to differentiate dysplasia from acquired forms of injury (Bernstein, 1992). We quantitated cell proliferation in *TgALK3<sup>QD/QD</sup>* kidney sections by counting the number of cells positive for Ki-67, a marker of proliferating cells (Tamamori-Adachi et al., 2003). Cell proliferation was increased sixfold and 17-fold in noncystic and cystic tubules, respectively, in the kidneys of homozygous Tg mice compared with tubules in the kidneys of control mice (Fig. 3A). Histological examination of tissue sections generated from the medulla of affected kidneys (Fig. 3B,C) revealed that the epithelial lining of many tubules had become

squamous in phenotype. Analysis of E-cadherin expression revealed an overall decrease in the amount of detectable protein in lysates generated from the kidneys of homozygous Tg mice. Decreased expression was observed in a subset of medullary tubules characterized by a columnar epithelium. E-cadherin expression was undetectable in tubules and cysts with a squamous epithelium (Fig. 3B). These changes were accompanied by a marked increase in MYC expression, which was observed in the nuclei of medullary tubules and cysts, particularly those characterized by a squamous epithelium (Fig. 3C). These results demonstrate tubular epithelial de-differentiation as a major feature of the renal phenotype in *TgALK3<sup>QD/QD</sup>* mice. Collectively, these findings are diagnostic of a dysplastic renal phenotype of embryonic origin similar to forms of human renal dysplasia in which severe disruption of medullary development co-exists with more limited abnormalities, including dilated cortical collecting ducts and decreased nephron number (Bernstein, 1992).

### Renal branching morphogenesis is decreased in *ALK3<sup>QD/QD</sup>* Tg mice

In the kidney, nephrogenesis is controlled by inductive interactions between the ureteric bud and the metanephric blastema. The number of nephrons formed is dependent on ureteric bud branching and other crucial factors, including survival of metanephric progenitor cells and integrity of the mesenchymal-epithelial transformation. Our observation that the number of medullary collecting tubules and cortical glomeruli was decreased in *TgALK3<sup>QD/QD</sup>* renal tissue suggested interruption of one or more of these crucial processes. The presence of both immature and mature glomeruli at E13.5-E18.5 did not support a defect in glomerular formation per se. However, our previous demonstration that the BMPs inhibit branching morphogenesis through ALK3 suggested that expression of an activated form of ALK3 could decrease branching morphogenesis. We analyzed such an effect by quantitating the number of ureteric bud branches at E13.5 in Tg and control mice. At this stage, branching morphogenesis is well established and discrete branch points can be identified using the ureteric bud specific marker DBA (Piscione et al., 1997). Quantitation of ureteric bud branch points demonstrated 30% fewer ureteric bud branches in kidneys of homozygous Tg mice compared with control mice (number of branch points, *TgALK3<sup>QD/QD</sup>* versus control:  $42.6 \pm 11.4$  versus  $65.1 \pm 15.3$ ,  $P < 0.01$ ; Fig. 4A). Interestingly, in ~25% of homozygous

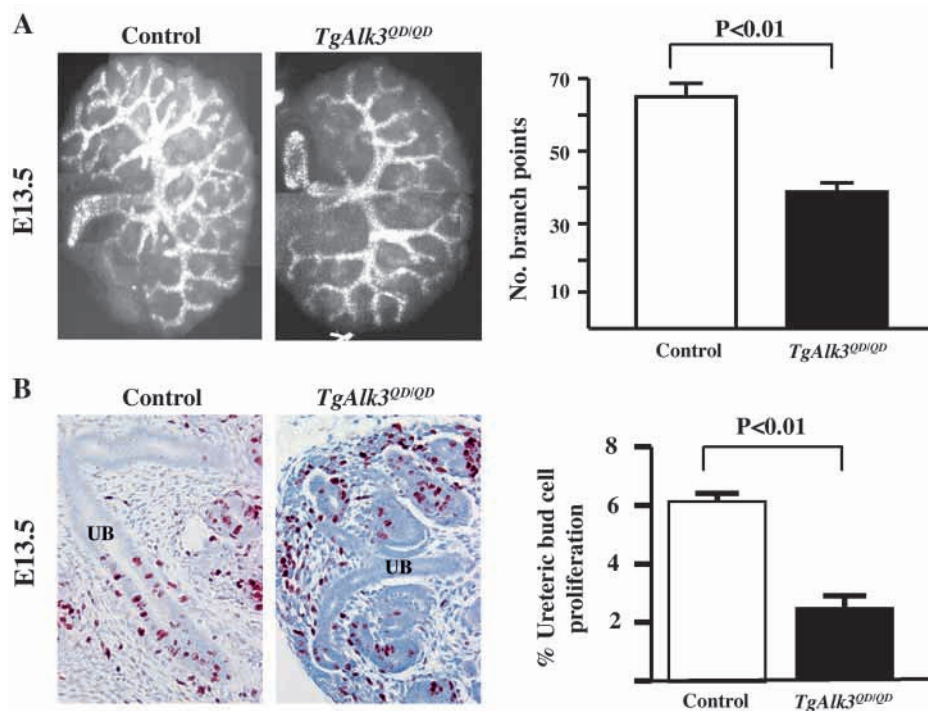


**Fig. 4.** Renal branching morphogenesis is reduced in kidneys from E13.5 *TgALK3<sup>QD/QD</sup>* embryos. (A) Ureteric bud branching in *TgALK3<sup>QD/QD</sup>* versus control kidneys. Left: DBA-stained whole-mount preparations of E13.5 kidneys. Ureteric bud branches are highlighted. Right: quantitation of branch points demonstrated 36% fewer branches in *TgALK3<sup>QD/QD</sup>* versus control kidneys. (B) Ureteric bud cell proliferation in *TgALK3<sup>QD/QD</sup>* versus control kidneys. Left: Hematoxylin-stained E13.5 kidney tissue. BrdU incorporation is identified by HRP-conjugated mouse anti-BrdU antibody yielding red colored cell nuclei. Note the marked reduction of BrdU uptake in the ureteric bud (UB) of *TgALK3<sup>QD/QD</sup>* mice. By contrast, BrdU in glomerular progenitors and mesenchymal cells is similar in *TgALK3<sup>QD/QD</sup>* and control kidney sections. Right: quantitation of the percentage of BrdU-positive ureteric bud cells demonstrated a 60% reduction in *TgALK3<sup>QD/QD</sup>* versus control mice. Data are mean  $\pm$  s.d from three separate experiments.

Tg mice, the number of branch points was within two standard deviations of the mean number observed in wild-type mice (data not shown). This observation is consistent with the variability of renal phenotype observed in other genetic mouse models (Srinivas et al., 1999b). As cell proliferation is fundamental to tubular growth and is controlled by BMP-dependent signaling (Piscione et al., 2001), we measured the incorporation of BrdU, a surrogate marker of cell proliferation, by ureteric bud cells (Fig. 4B). Our results indicate marked inhibition of ureteric bud cell proliferation in homozygous Tg mice (% BrdU-positive cells, control versus *TgALK3<sup>QD/QD</sup>*:  $6.1 \pm 0.6$  versus  $2.5 \pm 1.0$ ,  $P < 0.0001$ ). By contrast, no differences in BrdU incorporation into mesenchymal-derived DBA negative cells were observed and the formation of glomerular and tubular progenitors appeared normal at the histological level. These observations are consistent with our targeting of the transgene to the ureteric bud lineage and demonstrate inhibition of branching morphogenesis in *TgALK3<sup>QD</sup>* mice.

### Constitutive expression of activated ALK3 increases phospho-SMAD1 and $\beta$ -catenin expression in dysplastic renal tissue

We investigated the molecular mechanisms controlling the phenotypic transition from decreased ureteric bud cell proliferation and branching to increased cell proliferation and cystic dysplasia at later stages of renal development. First, we examined the activity of the ALK3 signaling pathway in the epithelium of dysplastic tissue using phospho-SMAD1 as a reporter. Like other type I BMP receptors, ALK3 signals via one or more members of the family of receptor-activated

SMAD proteins (Attisano and Wrana, 2000). In our previous work in collecting duct cells, we showed that ALK3 phosphorylates the receptor-activated SMAD, SMAD1 (Gupta et al., 1999), and that SMAD1 activity is required for the inhibitory functions of BMPs during branching morphogenesis (Piscione et al., 2001). Thus, we analyzed the expression of phosphorylated SMAD1 protein (phospho-SMAD1) as a cellular reporter of ALK3 activity using a specific antibody (Fig. 5). In contrast to control kidneys, phospho-SMAD1 was highly expressed in epithelial tubules and cysts located in the renal medulla of *TgALK3<sup>QD</sup>* mice (Fig. 5A). Phospho-SMAD1 was expressed at similar levels in glomeruli and proximal tubules in the kidney cortex of both control and transgenic mice (data not shown). These results were confirmed by analysis of whole kidney protein lysates with anti-SMAD1 antibodies. Analysis of immunoblots demonstrated that although SMAD1 was expressed in amounts that were not significantly different between control, hemizygous and homozygous Tg mice, significant increases in phospho-SMAD1 could be detected in hemizygous and homozygous Tg mice. These results indicate that ALK3 associated SMAD-dependent signaling is active in dysplastic renal tissue of *TgALK3<sup>QD</sup>* mice.

Recent studies demonstrate that BMPs control cellular processes by activating intracellular effectors in signaling pathways distinct from the SMAD pathway. For example, in cultured chondrocyte progenitors, BMPs can increase intracellular levels of  $\beta$ -catenin protein (Fischer et al., 2002a; Fischer et al., 2002b). Such an effect is of potential relevance to the pathogenesis of cystic renal dysplasia because  $\beta$ -catenin has been implicated in signaling events downstream of the

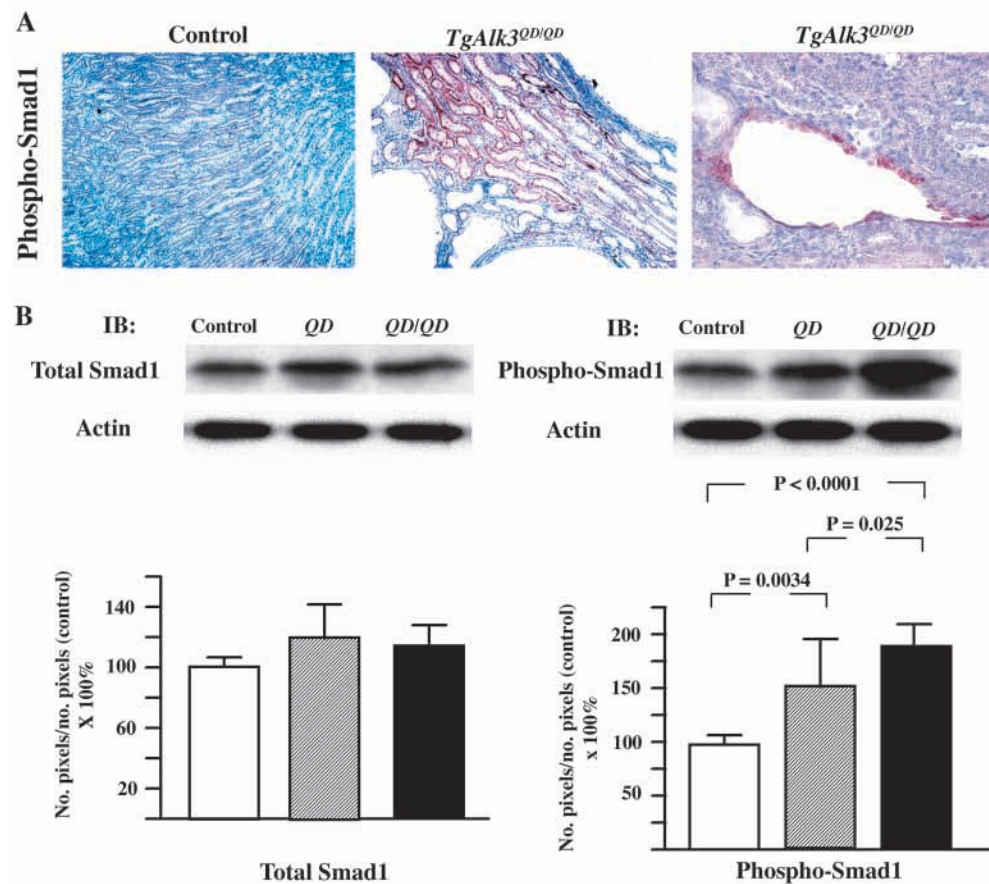


**Fig. 5.** Phospho-SMAD1 expression is increased in the P10 *TgALK3<sup>QD/QD</sup>* kidney.

(A) Phospho-SMAD1 expression in *TgALK3<sup>QD/QD</sup>* kidney. Left: Hematoxylin-stained control kidney tissue (medulla) stained with anti-phospho-SMAD1 antibody demonstrates very weak expression of phospho-SMAD1. Middle: Hematoxylin-stained tissue from a *TgALK3<sup>QD</sup>* mouse demonstrating a marked increase in phospho-SMAD1 expression. Right: Hematoxylin-stained tissue containing an epithelial cyst showing phospho-SMAD1 expression in cells lining the cyst. (B) Quantification of SMAD1 and phospho-SMAD1 protein expression in whole kidney lysate. Left: expression of total SMAD1 (unphosphorylated and phosphorylated) is similar in kidneys from control (white), *TgALK3<sup>QD</sup>* (QD; gray) and *TgALK3<sup>QD/QD</sup>* (QD/QD, black) mice. Right: phospho-SMAD1 expression is increased by 51% in *TgALK3<sup>QD</sup>* versus control kidney, and by 86% in *TgALK3<sup>QD/QD</sup>* kidneys. Representative blots are shown above. Data are mean  $\pm$  s.d. from four separate experiments.

autosomal dominant polycystic kidney disease gene polycystin 1 (Kim et al., 1999), and induces polycystic kidney disease when overexpressed in transgenic mice (Saadi-Kheddouci et al., 2001). To investigate the potential role of  $\beta$ -catenin during the pathogenesis of dysplasia in *TgALK3<sup>QD</sup>* mice, we measured the expression of  $\beta$ -catenin in kidney tissue sections and protein lysates (Fig. 6A).  $\beta$ -Catenin was not detected in tissue sections of neonatal control mice. By contrast,  $\beta$ -catenin expression was markedly increased in medullary epithelial tubules and cysts, but to a far lesser degree in the kidney cortex, of homozygous *Tg* mice. Within the renal medulla,  $\beta$ -catenin expression was heterogeneous. High levels of expression were observed in tubules and cysts with a cuboidal epithelium, but not generally in those with a squamous epithelium. This pattern of expression was similar to that observed for E-cadherin in *TgALK3<sup>QD</sup>* mice (Fig. 3B). Increased  $\beta$ -catenin expression was confirmed in tissue lysates in which a significant increase in  $\beta$ -catenin could be demonstrated in *TgALK3<sup>QD</sup>* mice. Because stabilization of cytoplasmic  $\beta$ -catenin is regulated by WNT signaling (Miller, 2002), we investigated whether enhanced expression of WNT

family members is associated with the increase in  $\beta$ -catenin. Analysis of mRNAs encoding WNT11, WNT4, WNT2B, WNT5B, WNT7B and WNT6, all of which are expressed in kidney (Vainio and Uusitalo, 2000), did not demonstrate any association between the expression of these WNTs and the dysplastic phenotype (data not shown).

Genetic interactions between the BMP and WNT pathways have been previously observed in non-renal tissues in invertebrates (Riese et al., 1997), lower vertebrates (Hoppler and Moon, 1998; Nishita et al., 2000) and cultured cells (Fischer et al., 2002a; Fischer et al., 2002b; Labbe et al., 2000). We investigated these interactions in vivo by generating *QD/QD*; *Tcf-gal* mice. The *Tcf-gal* mouse is a model reporter of the transcriptional activity of  $\beta$ -catenin in partnership with members of the TCF family (Cheon et al., 2002). Expression of  $\beta$ -galactosidase by *lacZ* is controlled by a FOS minimal promoter and three consensus TCF-binding motifs. We detected low levels of  $\beta$ -galactosidase activity in tubular epithelium resident in the renal cortex of *Tcf-gal* mice (Fig. 6B). By contrast, we observed a remarkable enhancement of *lacZ* transcription activity in *QD/QD*; *Tcf-gal* mice (Fig. 6B).

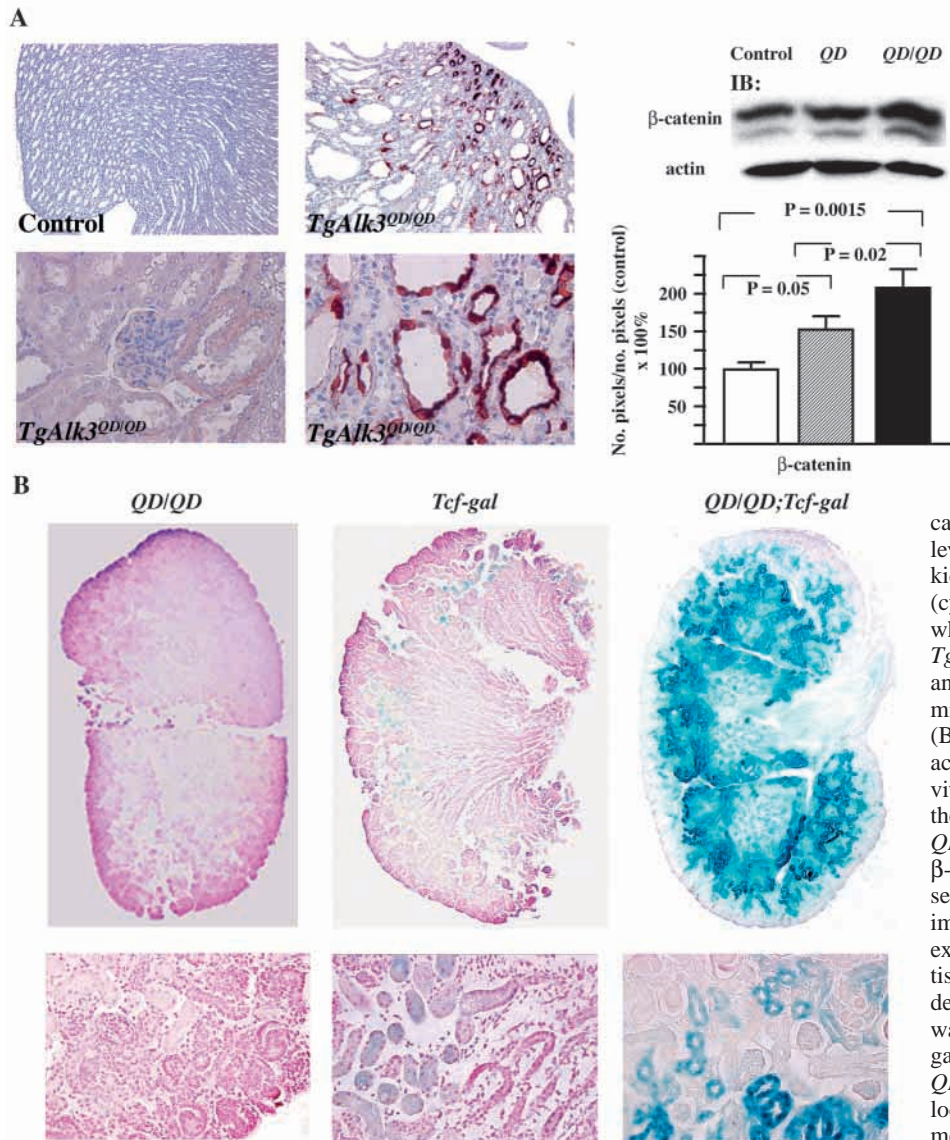


**Fig. 6.**  $\beta$ -catenin is increased in postnatal *TgALK3<sup>QD/QD</sup>* mouse kidney tissue. (A) Immunohistochemistry of kidney tissue from control and *TgALK3<sup>QD/QD</sup>* mice at P10, using rabbit anti-human  $\beta$ -catenin and HRP-conjugated anti-rabbit antibodies. Top left panels: Hematoxylin-stained kidney tissue from control mouse demonstrates absence of detectable  $\beta$ -catenin protein in the medulla. Hematoxylin-stained kidney tissue from *TgALK3<sup>QD/QD</sup>* mouse demonstrates marked upregulation of  $\beta$ -catenin expression in a subset of tubules and epithelial cysts in the medulla. Bottom left panels: higher power view of kidney cortex of a *TgALK3<sup>QD/QD</sup>* mouse. Low levels of  $\beta$ -catenin were detected. By contrast,  $\beta$ -catenin levels in the medulla of a *TgALK3<sup>QD/QD</sup>* mouse kidney are greatly increased in dilated tubules (cysts). Right panel:  $\beta$ -catenin expression in whole kidney lysate was increased by 46% in *TgALK3<sup>QD</sup>* (gray) versus control (white) mice, and by a further 60% in *TgALK3<sup>QD/QD</sup>* (black) mice. A representative blot is shown above. (B) Activation of ALK3 signaling increases the activity of a  $\beta$ -catenin/TCF reporter gene in vivo.  $\beta$ -galactosidase activity was assayed in the kidneys of newborn *QD/QD*, *Tcf-gal* and *QD/QD*; *Tcf-gal* mice. Top panels demonstrate  $\beta$ -gal expression in Eosin-stained cross-sections of the entire kidney (composite image). Lower panels demonstrate  $\beta$ -gal expression in representative corresponding tissue sections. No  $\beta$ -gal expression was detected in *QD/QD* kidneys. Weak expression was detected in *Tcf-gal* mice. By contrast,  $\beta$ -gal expression was markedly increased in *QD/QD*; *Tcf-gal* mouse kidney, with localization in tubular epithelium. Data are mean  $\pm$  s.d. from three independent experiments.

These data demonstrate genetic interactions between the ALK3 and  $\beta$ -catenin signaling pathways in kidney tissue.

### Association of Phospho-SMAD1 and $\beta$ -catenin in molecular complexes is increased in dysplastic *TgALK3<sup>QD</sup>* mouse kidney

Molecular interactions between the  $\beta$ -catenin binding partner, LEF1/TCF, and the TGF- $\beta$  SMAD signaling effectors, SMAD2, SMAD3 and SMAD4 have been demonstrated in *Xenopus* (Nishita et al., 2000) and cultured mammalian cells (Fischer et al., 2002a; Labbe et al., 2000). By contrast, no interactions between SMAD1 and  $\beta$ -catenin or TCF have yet been demonstrated. Our finding of increased transcriptional activity in *QD/QD*; *Tcf-gal* mice suggested possible molecular interactions between ALK3 signaling effectors and  $\beta$ -catenin. We investigated interactions between SMAD1, SMAD4 and  $\beta$ -catenin in renal tissue lysates isolated from P10 mice by co-immunoprecipitation and immunoblotting (Fig. 7). Whereas low levels of  $\beta$ -catenin were detected in association with SMAD1 in the renal tissue of controls,  $\beta$ -catenin levels associated with SMAD1 were increased ninefold in kidney

lysates from homozygous *Tg* mice (Fig. 7A). Similarly, a ninefold elevation of phospho-SMAD1 in association with  $\beta$ -catenin was also detected in homozygous *Tg* mouse kidney compared with that of controls (Fig. 7B). Formation of molecular complexes between phospho-SMAD1 and the common SMAD, SMAD4, before translocation to the nucleus, suggested that elevated levels of phospho-SMAD1 associated with  $\beta$ -catenin would be accompanied by increased amounts of SMAD4. Our results indicate a twofold elevation in levels of SMAD4 associated with  $\beta$ -catenin (Fig. 7C). Compared with SMAD1, the lower amount of SMAD4 associated with  $\beta$ -catenin suggests that the ratio of SMAD4:SMAD1 may not be 1:1 in molecular complexes containing of  $\beta$ -catenin, and that SMAD1/ $\beta$ -catenin complexes may function in a manner distinct from those containing SMAD4. Taken together, these results are the first demonstration of molecular associations among SMAD1, SMAD4 and  $\beta$ -catenin during the genesis of dysplasia during mammalian organogenesis.

### The levels of phospho-SMAD1 and $\beta$ -catenin are increased in human renal dysplastic tissue

Human renal dysplasia is a pleiomorphic and poorly understood disorder that consists of numerous histopathological subtypes. At the most severe end of the spectrum is agenesis and severe multicystic dysplasia. The histology of these tissues indicates a total, or near-total, interruption of inductive tissue interactions and subsequent formation of ureteric bud- and blastema-derived epithelial tissue elements. A more intermediate phenotype, frequently associated with congenital dilatation of the lower urinary tract, consists of a preserved corticomedullary pattern, a hypoplastic cortex with cysts, dilated collecting ducts, a decrease in the number of collecting ducts, and increased mesenchyme in the medulla (Daikha-Dahmane et al., 1997). The similarity between this phenotype and that observed in *TgALK3<sup>QD</sup>* mice, suggests that pathogenic mechanisms may be shared. Thus, we studied, by immunohistochemistry, the expression of phospho-SMAD1 and  $\beta$ -catenin in normal and dysplastic 20-22-week fetal kidney tissue (Fig. 8). Whereas normal tissue consisted of a well organized and complete complement of epithelial structures (Fig. 8A,D,G), dysplastic tissue was characterized by disorganization of tissue elements, a marked decrease in the number of tubules (Fig. 8E,F) and formation of epithelial cysts derived from the ureteric bud lineage (Fig. 8H,I). Although phospho-SMAD1 was undetectable in normal tissue (Fig. 8A), it was highly expressed in the ureteric bud (Fig. 8B) and in epithelial cysts (Fig. 8C). Similarly, expression of  $\beta$ -catenin was elevated in dysplastic tissue compared with normal tissue (Fig. 8D-I). These data demonstrate dysregulation of phospho-SMAD1 and  $\beta$ -catenin in human renal dysplasia.

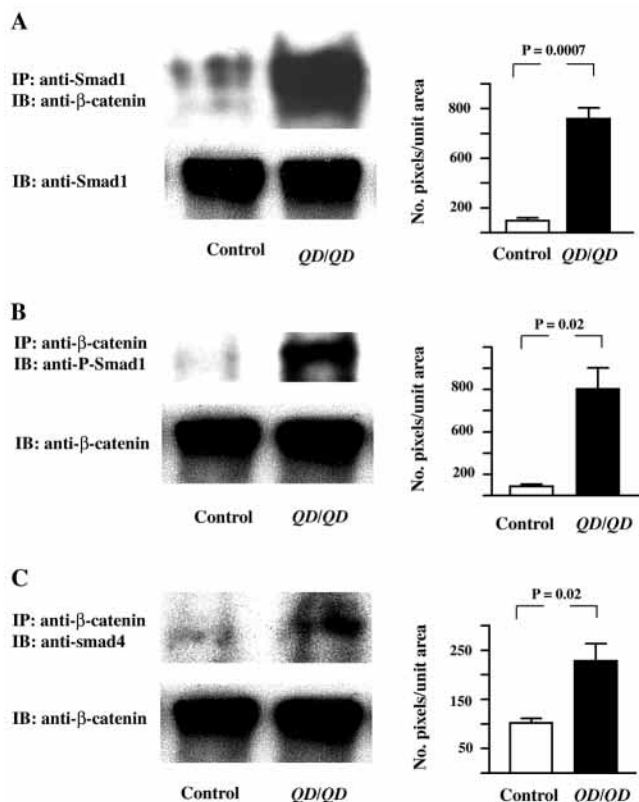


**Fig. 7.** SMAD1 and  $\beta$ -catenin are associated in molecular complexes in *TgALK3<sup>QD/QD</sup>* (*QD/QD*) mice. Molecular associations in postnatal kidney tissue (P10) isolated from different mice were assayed by immunoprecipitation-immunoblot assays using specific antisera. Immunoblots and quantitation are shown in the left and right panels, respectively. (A) The amount of  $\beta$ -catenin associated with SMAD1 was increased ninefold in *Tg* mice versus controls. (B) The amount of phospho-SMAD1 associated with  $\beta$ -catenin was increased ninefold in *Tg* mice versus controls. (C) The amount of SMAD4 associated with  $\beta$ -catenin was increased twofold in *Tg* mice versus controls. Data are mean  $\pm$  s.d. from three independent experiments.

## DISCUSSION

### A novel murine model of renal medullary cystic dysplasia

As a group of human developmental disorders, phenotypic subtypes of renal dysplasia vary by the particular tissue elements that are malformed and in the severity of these perturbations. Despite extensive information available regarding gene expression in the embryonic kidney, perhaps not

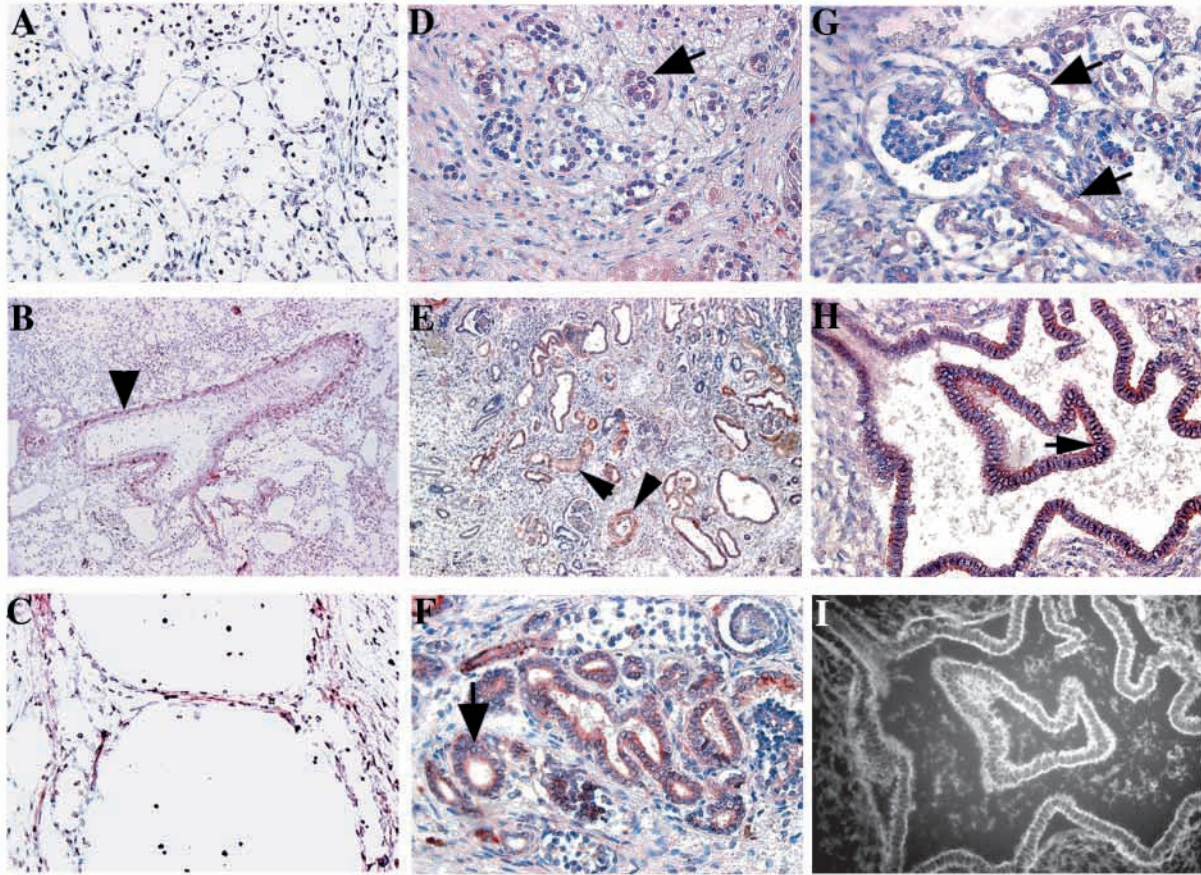


**Fig. 8.** Phospho-SMAD1 and  $\beta$ -catenin expression is increased in human dysplastic fetal kidney. (A–C) Phospho-SMAD1 expression detected by immunohistochemistry using anti-phospho-SMAD1 and HRP-conjugated secondary antibodies. (A) Phospho-SMAD1 is undetectable in normal Hematoxylin-stained tissue. (B) Phospho-SMAD1 is markedly unregulated in Hematoxylin-stained dysplastic tissue (red cells), including a branched ureteric bud (arrowhead) and in cysts (C). (D–I)  $\beta$ -catenin expression detected by immunohistochemistry using anti- $\beta$ -catenin and HRP-conjugated secondary antibodies. (D,G)  $\beta$ -catenin is weakly expressed in epithelial tubules (arrows) of Hematoxylin-stained normal kidney tissue. (E,F)  $\beta$ -catenin is highly expressed in epithelial tubules (arrows) of Hematoxylin-stained dysplastic kidney tissue. (H,I)  $\beta$ -catenin is highly expressed in the epithelium of ureteric bud-derived cysts. (H)  $\beta$ -catenin is highly expressed in cyst epithelium (arrow). (I) Fluorescence image of cyst in H stained with fluorescence-conjugated DBA. Positive staining demonstrates that the cyst is derived from the ureteric bud.

unexpectedly, analysis of most mutant phenotypes has provided insight into the pathogenesis of the more severe forms of renal dysplasia, i.e. renal aplasia and renal dysgenesis (reviewed by Piscione and Rosenblum, 1999; Pohl et al., 2002). Analyses of mice with naturally occurring or engineered mutations have demonstrated crucial functions for transcription factors [PAX2, LIM1 (LHX1 – Human Gene Nomenclature Database), SALL1, RARs], growth factors (GDNF, WNT4, BMP4, BMP7), growth factor receptors (RET, GFR $\alpha$ 1), integrins ( $\alpha$ 8 integrin) and heparan sulfation (HS2ST) during the reciprocal inductive interactions required for branching morphogenesis and the mesenchymal-epithelial transformation.

A subset of human renal dysplasias is characterized by less severe abnormalities that are either more focal in spatial distribution, or are restricted to one or more tissue elements, such as medullary collecting ducts. Because the tissue damage in these phenotypes is less pervasive and severe, they are associated with some degree of renal survival during fetal and postnatal life. With a view towards human disease, it is crucial to understand the pathogenesis of these forms of dysplasia

because the knowledge gained may lead to strategies aimed at modifying aberrant developmental pathways and ameliorating disease. In this paper, we report a mouse model of medullary cystic dysplasia in which nephrogenesis is qualitatively intact but quantitatively deficient, and in which decreased branching morphogenesis is associated with a decreased mass of medullary collecting ducts and with cystic degeneration of these tubules.

The renal phenotype of *TgALK3<sup>QD</sup>* mice is distinct from that of other mouse models characterized by misdevelopment of the renal medulla. These include mice deficient for angiotensinogen (*Ang*), angiotensin receptor-1 (*Agtr1*) and -2 (*Agtr2*), glypican 3 (*Gpc3*), p57<sup>KIP2</sup> and BMP4. *Ang*<sup>−/−</sup> and *Agtr1*<sup>−/−</sup> mice demonstrate progressive dilatation of the calyx, and atrophy of the papilla and underlying medulla after birth. These defects appear to be caused by decreased proliferation of the smooth muscle layer lining the pelvis, which results in decreased thickness of this layer in the proximal ureter (Miyazaki et al., 1998; Niimura et al., 1995). *Agtr2* inactivation results in a spectrum of renal dysplasia and lower urinary tract

abnormalities termed CAKUT. These malformations appear to be caused by misdevelopment of the proximal ureter and by secondary effects on the development of the renal parenchyma (Nishimura et al., 1999). GPC3 deficiency causes medullary cystic dysplasia owing to massive apoptosis of medullary collecting ducts. In contrast to *TgALK3<sup>QD</sup>* mice, in *Gpc3*-mutant mice, medullary dysplasia is preceded by an increase in branching morphogenesis and ureteric bud cell proliferation (Cano-Gauci et al., 1999; Grisaru et al., 2001). The renal phenotype of *p57<sup>KIP2</sup>*-null mice is similar to that observed in *Gpc3*-null mice. Although the pathogenic mechanisms have not been elucidated, the function of *p57<sup>KIP2</sup>* as an inhibitor of cyclin-dependent kinases suggests that it may act in a pathway shared by *Gpc3*. Although *Bmp4*, a *Bmp2* homolog, can signal through ALK3, *Bmp4*<sup>+/-</sup> mice exhibit a phenotype distinct from that observed in *TgALK3<sup>QD</sup>* mice. Renal dysplasia in *Bmp4*<sup>+/-</sup> mice appears to be caused by abnormal budding of the ureteric bud at its origin at the Wolffian Duct, and, consequently, abnormal interactions between one or more ureteric buds and the metanephric blastema (Miyazaki et al., 2000). This, in turn, results in focal dysplasia consisting of a major interruption of nephrogenesis with cystic dysplasia and hydronephrosis. Thus, the unique renal phenotype observed in *TgALK3<sup>QD</sup>* mice suggests the existence of novel pathogenic mechanisms not previously discovered in other models of renal dysplasia. The similarity of this phenotype to that observed in some fetuses with associated lower urinary tract dilatation suggests that knowledge of these mechanisms will provide further insight into the pathogenesis of human dysplasia (Al Saadi et al., 1984; Daikha-Dahmane et al., 1997).

### ALK3 inhibits renal branching morphogenesis

The invariant structural organization of the mature kidney and the relatively constant number of collecting ducts formed suggests that branching morphogenesis is a tightly regulated process. We have hypothesized that regulation of renal branching morphogenesis occurs through the integrated actions of stimulatory signaling pathways, including GDNF/RET, and inhibitory pathways downstream of BMP2 and its receptor ALK3 (Piscione et al., 1997). *Bmp2* is expressed in the metanephric mesenchyme adjacent to the tips of ureteric bud branches (Dudley and Robertson, 1997). *Alk3* is expressed in both ureteric bud and blastemal cells during early stages of renal development, and at lower levels later during gestation. Identification of the roles played by BMP2 and ALK3 has been limited by the early embryonic lethality induced by mutational inactivation of either gene. Although deletion of one allele of the BMP2 homolog BMP4 gives rise to a dysplastic renal phenotype, the distinct pattern of BMP4 expression in the mesenchyme surrounding the Wolffian Duct and the ureteric bud (Miyazaki et al., 2000) suggests a function different from that of BMP2, and limits speculation regarding the function of ALK3 in regions adjacent to *Bmp2* expression. Previously, we demonstrated that BMP2 and ALK3 inhibit renal branching morphogenesis in embryonic kidney explants and in a 3-dimensional culture model of tubule formation. Our results in the *TgALK3<sup>QD</sup>* mouse are consistent with these results and provide the first demonstration in vivo that activation of ALK3 in the ureteric bud inhibits branching morphogenesis. This effect probably underlies the pathogenesis of renal aplasia in a small group of *TgALK3<sup>QD</sup>* mice. The relatively small number

of mice with this malformation may be because of modifying factors, including the level of expression of the transgene and the genetic background of the mice. Indeed, our results demonstrated considerable variation in the effect on branch point number within progeny derived from the same founder. In the majority of *TgALK3<sup>QD</sup>* mice, the inhibitory effect of ALK3<sup>QD</sup> is insufficient to abrogate ureteric bud growth. Rather, it inhibits branching, thereby inducing hypoplasia of the collecting system and decreasing the number of nephrons induced. Recognition of this effect suggests that ALK3 activity must be tightly regulated. The basis for this regulation remains unknown. Because the *ALK3<sup>QD</sup>* transgene was mainly expressed in the ureteric bud lineage, we are unable to interpret the role of ALK3 in the metanephric mesenchyme. The development of mice expressing *Cre* recombinase in specific kidney cell lineages under temporal control will provide a means to study the actions of ALK3 in the ureteric bud and metanephric blastema both separately and together.

### Interactions between the BMP and WNT pathways during organogenesis

Our analysis of *TgALK3<sup>QD</sup>* mice revealed genetic and molecular interactions between effectors in the BMP and WNT pathways. Our data expand the breadth of interactions previously observed during embryogenesis in flies and frogs, and during tumor formation in mice. In *Drosophila*, *dpp*, a BMP2/4 homolog, and *wg*, a WNT homolog, act synergistically to regulate the expression of ultrabithorax (*Ubx*) in the endoderm (Riese et al., 1997). In *Xenopus*, SMAD4 and LEF1 cooperate to control the expression of the homeobox gene *Xtwn8* in Spemann's organizer (Nishita et al., 2000). In mice, deficiency of one *Smad4* allele synergizes with deficiency of APC, a regulator of  $\beta$ -catenin degradation, to increase the number and invasiveness of intestinal tumors (Takaku et al., 1998). These findings have been extended to the level of molecular interactions in *Xenopus* by the demonstration of SMAD4/LEF1(TCF) and SMAD4/ $\beta$ -catenin molecular complexes, and the cooperative interaction of SMAD4 and LEF1/TCF at the XTWN promoter (Nishita et al., 2000). These nature of these interactions has been further defined by the demonstration that LEF1/TCF binds via its C-terminal domain to the TGF- $\beta$  effectors SMAD2, SMAD3 and SMAD4 (Labbe et al., 2000). Our results reveal interactions between  $\beta$ -catenin and SMAD1, implicating the BMP pathway in interactions with this WNT effector. Although data reveal that these pathways interact cooperatively at the level of a *Tcf* reporter in kidney tissue, further experiments will be required to identify the functional consequences of SMAD1/ $\beta$ -catenin interactions. The recognition that the MYC promoter contains SMAD-binding elements as well as TCF-binding elements (Yagi et al., 2002) provides a basis for studying these interactions in the context of a gene that is relevant to the pathogenesis of polycystic kidney disease (Trudel et al., 1998) and cystic dysplasia (our data).

### Interactions between the BMP and WNT pathways during the genesis of renal disease

Our data from *TgALK3<sup>QD</sup>* mice indicate that ALK3 upregulates  $\beta$ -catenin expression. Previous observations demonstrating that  $\beta$ -catenin is upregulated by polycystin 1, the gene product mutated in type I autosomal dominant polycystic kidney

disease (Kim et al., 1999), and that  $\beta$ -catenin induces polycystic kidney disease when overexpressed in transgenic mice (Saadi-Kheddouci et al., 2001) suggest that dysregulation of BMP signaling in the embryonic kidney triggers a cystogenic pathway. Similarly, these findings, together with those presented here, raise the possibility of dysregulation of the BMP pathway in polycystic kidney disease. The mechanisms mediating interactions between ALK3 and  $\beta$ -catenin remain to be determined. One possibility is that BMP signaling upregulates WNT expression, a positive effector of  $\beta$ -catenin expression. Although we were not able to associate the expression of a subset of WNT proteins with ALK3 signaling in vivo, one or more of the larger number of WNTs may be involved in this process. Alternatively, ALK3 may control  $\beta$ -catenin signaling in a manner that is WNT-independent. The BMP family member TGF- $\beta$  controls cytoplasmic levels of  $\beta$ -catenin in cultured cells by stimulating redistribution of  $\beta$ -catenin from adherens junctions to the cytoplasm (Tian and Phillips, 2002). BMP-dependent activation of MAP kinases, such as TAK1 (MAP3K7 – Human Gene Nomenclature Database), control  $\beta$ -catenin signaling at the level of transcription. TAK1 is an intracellular target of TGF- $\beta$  and BMPs (Yamaguchi et al., 1995), and is required for BMP-dependent control of cardiomyocyte differentiation (Monzen et al., 2001). Acting through its downstream targets, TAK1 modulates the transcriptional activity of  $\beta$ -catenin/TCF molecular complexes (Ishitani et al., 1999). Taken together with our observations, these observations provide a basis for identifying BMP-dependent molecules that modulate the intracellular levels of  $\beta$ -catenin and/or its transcriptional activity in conjunction with TCF family members.

Our findings provide a basis for generating a two-phase model of medullary renal dysplasia caused by expression of activated ALK3 in the ureteric bud lineage. In the first phase, inhibition of branching morphogenesis inhibits nephron formation, leading to the formation of a thin outer cortex. During the second phase, ALK3 upregulates  $\beta$ -catenin, alters the expression of genes crucial for epithelial cell differentiation and induces cystogenesis. Further experiments will be required to determine the specific elements of this model. These will include strategies to test the effect of SMAD1/ $\beta$ -catenin complexes on the expression of genes such as E-cadherin and *MYC*, and the development of new mouse models in which the expression of  $\beta$ -catenin is temporally and spatially controlled in the kidney. These approaches will need to be complemented by the analysis of a broad range of phenotypes in tissue samples taken from individuals with renal dysplasia to gain further insight into the general significance of our finding that phospho-SMAD1 and  $\beta$ -catenin are markedly upregulated in dysplastic renal tissues.

The authors thank Drs L. Attisano, F. Costantini, J. Ellis, C.-C. Hui and H. Lipshitz for helpful discussions during the course of this work. This research was supported by grants from the Canadian Institutes of Health Research (to N.D.R.) and by a Canadian Society of Nephrology/Kidney Foundation of Canada Fellowship (to T.D.P.).

## REFERENCES

- Al Saadi, A. A., Yoshimoto, M., Bree, R., Farah, J., Chang, C.-H., Sahney, S., Shokeir, M. H. K. and Bernstein, J. (1984). A family study of renal dysplasia. *Am. J. Med. Genet.* **19**, 669-677.
- Attisano, L. and Wrana, J. L. (2000). Smads as transcriptional co-modulators. *Curr. Opin. Cell Biol.* **12**, 235-243.
- Bernstein, J. (1992). Renal hypoplasia and dysplasia. In *Pediatric Kidney Disease* (ed. J. Bernstein, C. M. Edelmann, S. R. Meadow, A. Spitzer and L. B. Travis), pp. 1121-1137. Boston, MA: Little, Brown and Co.
- Cano-Gauci, D. F., Song, H. H., Yang, H., McKerlie, C., Choo, B., Shi, W., Pullano, R., Piscione, T. D., Grisaru, S., Soon, S. et al. (1999). Glypican-3-deficient mice exhibit the overgrowth and renal abnormalities typical of the Simpson-Golabi-Behmel syndrome. *J. Cell Biol.* **146**, 255-264.
- Cheon, S. S., Cheah, A. Y., Turley, S., Nadesan, P., Poon, R., Clevers, H. and Alman, B. A. (2002).  $\beta$ -Catenin stabilization dysregulates mesenchymal cell proliferation, motility, and invasiveness and causes aggressive fibromatosis and hyperplastic cutaneous wounds. *Proc. Natl. Acad. Sci. USA* **99**, 6973-6978.
- Daïkha-Dahmane, F., Dommergues, M., Muller, F., Narcy, F., Lacoste, M., Beziau, A., Dumez, Y. and Gubler, M.-C. (1997). Development of human fetal kidney in obstructive uropathy: correlations with ultrasonography and urine biochemistry. *Kidney Int.* **52**, 21-32.
- Dewulf, N., Verschuere, K., Lonnoy, O., Morén, A., Grimsby, S., Vande Spiegle, K., Miyazono, K., Huylebrouck, D. and Ten Dijke, P. (1995). Distinct spatial and temporal expression patterns of two type 1 receptors for bone morphogenetic proteins during mouse embryogenesis. *Endocrinology* **136**, 2652-2663.
- Dudley, A. T. and Robertson, E. J. (1997). Overlapping expression domains of bone morphogenetic protein family members potentially account for limited tissue defects in BMP7 deficient embryos. *Dev. Dyn.* **208**, 349-362.
- Fischer, L., Boland, G. and Tuan, R. S. (2002a). Wnt signaling during BMP-2 stimulation of mesenchymal chondrogenesis. *J. Cell. Biochem.* **84**, 816-831.
- Fischer, L., Boland, G. and Tuan, R. S. (2002b). Wnt-3A enhances BMP-2 mediated chondrogenesis of murine C3H10T1/2 mesenchymal cells. *J. Biol. Chem.* **277**, 30870-30878.
- Flanders, K. C., Kim, E. S. and Roberts, A. B. (2001). Immunohistochemical expression of Smads 1-6 in the 15-day gestation mouse embryo: signaling by BMPs and TGF- $\beta$ s. *Dev. Dyn.* **220**, 141-154.
- Godin, R. E., Takaesu, N. T., Robertson, E. J. and Dudley, A. T. (1998). Regulation of BMP7 expression during kidney development. *Development* **125**, 3473-3482.
- Grisaru, S., Cano-Gauci, D., Tee, J., Filmus, J. and Rosenblum, N. D. (2001). Glypican-3 modulates BMP- and FGF-mediated effects during renal branching morphogenesis. *Dev. Biol.* **230**, 31-46.
- Gupta, I. R., Piscione, T. D., Grisaru, S., Phan, T., Macias-Silva, M., Zhou, X., Whiteside, C., Wrana, J. L. and Rosenblum, N. D. (1999). Protein Kinase A is a negative regulator of renal branching morphogenesis and modulates inhibitory and stimulatory bone morphogenetic proteins. *J. Biol. Chem.* **274**, 26305-26314.
- Gupta, I. R., Macias-Silva, M., Kim, S., Zhou, X., Piscione, T. D., Whiteside, C., Wrana, J. L. and Rosenblum, N. D. (2000). HGF rescues BMP-2-mediated inhibition of renal collecting duct morphogenesis without interrupting Smad1 dependent signaling. *J. Cell Sci.* **113**, 269-278.
- Hoodless, P. A., Haerry, T., Abdollah, S., Stapleton, M., O'Connor, M. B., Attisano, L. and Wrana, J. L. (1996). MADR1, a MAD-related protein that functions in BMP2 signaling pathways. *Cell* **85**, 489-500.
- Hoppler, S. and Moon, R. T. (1998). BMP-2/-4 and Wnt-8 cooperatively pattern the *Xenopus* mesoderm. *Mech. Dev.* **71**, 119-129.
- Ishitani, T., Ninomiya-Tsuji, J., Nagai, S., Nishita, M., Meneghini, M., Barker, N., Waterman, M., Bowerman, B., Clevers, H., Shibuya, H. et al. (1999). The TAK1-NLK-MAPK-related pathway antagonizes signalling between  $\beta$ -catenin and transcription factor TCF. *Nature* **399**, 798-802.
- Kim, E., Arnould, T., Sellin, L. K., Benzing, T., Fan, M. J., Gruning, W., Sokol, S. Y., Drummond, I. and Walz, G. (1999). The polycystic kidney disease 1 gene product modulates Wnt signaling. *J. Biol. Chem.* **274**, 4947-4953.
- Kress, C., Vogels, R., De Graaff, W., Bonnerot, C., Meijlink, F., Nicolas, J.-F. and Deschamps, J. (1990). Hox-2.3 upstream sequences mediate lacZ expression in intermediate mesoderm derivatives of transgenic mice. *Development* **109**, 775-786.
- Labbe, E., Letamendia, A. and Attisano, L. (2000). Association of Smads with lymphoid enhancer binding factor 1/T cell-specific factor mediates cooperative signaling by the transforming growth factor- $\beta$  and Wnt pathways. *Proc. Natl. Acad. Sci. USA* **97**, 8358-8363.
- Miller, J. R. (2002). The Wnts. *Genome Biol.* **3**, R3001.
- Mishina, Y. A., Susuki, A., Ueno, N. and Behringer, R. R. (1995). BMP-

- encodes a type I bone morphogenetic protein receptor that is essential for gastrulation during mouse embryogenesis. *Genes Dev.* **9**, 3027-3037.
- Miyazaki, Y., Tsuchida, S., Nishimura, H., Pope, J. C., IV, Harris, R. C., McKanna, J. M., Inagami, T., Hogan, B. L. M., Fogo, A. and Ichikawa, I. (1998). Angiotensin induces the urinary peristaltic machinery during the perinatal period. *J. Clin. Invest.* **102**, 1489-1497.
- Miyazaki, Y., Oshima, K., Fogo, A., Hogan, B. L. and Ichikawa, I. (2000). Bone morphogenetic protein 4 regulates the budding site and elongation of the mouse ureter. *J. Clin. Invest.* **105**, 863-873.
- Monzen, K., Hiroi, Y., Kudoh, S., Akazawa, H., Oka, T., Takimoto, E., Hayashi, D., Hosoda, T., Kawabata, M., Miyazono, K. et al. (2001). Smads, TAK1, and their common target ATF-2 play a critical role in cardiomyocyte differentiation. *J. Cell Biol.* **153**, 687-698.
- Neu, A. M., Ho, P. L., McDonald, R. A. and Warady, B. A. (2002). Chronic dialysis in children and adolescents. The 2001 NAPRTCS Annual Report. *Pediatr. Nephrol.* **17**, 656-663.
- Newman, J. H., Wheeler, L., Lane, K. B., Loyd, E., Gaddipati, R., Phillips, J. A., 3rd and Loyd, J. E. (2001). Mutation in the gene for bone morphogenetic protein receptor II as a cause of primary pulmonary hypertension in a large kindred. *N. Engl. J. Med.* **345**, 319-324.
- Niimura, F., Labostky, P. A., Kakuchi, J., Okubo, S., Yoshida, H., Oikawa, T., Ichiki, T., Naftilan, A. J., Fogo, A., Inagami, T. et al. (1995). Gene targeting in mice reveals a requirement for angiotensin in the development and maintenance of kidney morphology and growth factor regulation. *J. Clin. Invest.* **96**, 2947-2954.
- Nishimura, H., Yerkes, E., Hohenfellner, K., Miyazaki, Y., Ma, J., Hunley, T. E., Yoshida, H., Ichiki, T., Threadgill, D., Phillips, J. A. et al. (1999). Role of the angiotensin type 2 receptor gene in congenital anomalies of the kidney and urinary tract, CAKUT, of mice and men. *Mol. Cell* **3**, 1-10.
- Nishita, M., Hashimoto, M. K., Ogata, S., Laurent, M. N., Ueno, N., Shibuya, H. and Cho, K. W. (2000). Interaction between Wnt and TGF- $\beta$  signalling pathways during formation of Spemann's organizer. *Nature* **403**, 781-785.
- Piscione, T. D. and Rosenblum, N. D. (1999). The malformed kidney: disruption of glomerular and tubular development. *Clin. Genet.* **56**, 343-358.
- Piscione, T. D., Yager, T. D., Gupta, I. R., Grinfeld, B., Pei, Y., Attisano, L., Wrana, J. L. and Rosenblum, N. D. (1997). BMP-2 and OP-1 exert direct and opposite effects on renal branching morphogenesis. *Am. J. Physiol.* **273**, F961-F975.
- Piscione, T. D., Phan, T. and Rosenblum, N. D. (2001). BMP7 controls collecting tubule cell proliferation and apoptosis via Smad1-dependent and -independent pathways. *Am. J. Physiol. Renal Physiology* **280**, F19-F33.
- Pohl, M., Bhatnagar, V., Mendoza, S. A. and Nigam, S. K. (2002). Toward an etiological classification of developmental disorders of the kidney and upper urinary tract. *Kidney Int.* **61**, 10-19.
- Riese, J., Yu, X., Munnerlyn, A., Eresh, S., Hsu, S. C., Grosschedl, R. and Bienz, M. (1997). LEF-1, a nuclear factor coordinating signaling inputs from wingless and decapentaplegic. *Cell* **88**, 777-787.
- Saadi-Kheddouci, S., Berrebi, D., Romagnolo, B., Cluzeaud, F., Peuchmaur, M., Kahn, A., Vandewalle, A. and Perret, C. (2001). Early development of polycystic kidney disease in transgenic mice expressing an activated mutant of the  $\beta$ -catenin gene. *Oncogene* **20**, 5972-5981.
- Saxen, L. (1987). Organogenesis of the kidney. Cambridge: Cambridge University Press.
- Srinivas, S., Goldberg, M. R., Watanabe, T., D'Agati, V., Al-Awqati, Q. and Costantini, F. (1999a). Expression of green fluorescent protein in the ureteric bud of transgenic mice: a new tool for the analysis of ureteric bud morphogenesis. *Dev. Genet.* **24**, 241-251.
- Srinivas, S., Wu, Z., Chen, C.-M., D'Agati, V. and Costantini, F. (1999b). Dominant effects of RET receptor misexpression and ligand-independent RET signaling on ureteric bud development. *Development* **126**, 1375-1386.
- Takaku, K., Oshima, M., Miyoshi, H., Matsui, M., Seldin, M. F. and Taketo, M. M. (1998). Intestinal tumorigenesis in compound mutant mice of both Dpc4 (Smad4) and Apc genes. *Cell* **92**, 645-656.
- Tamamori-Adachi, M., Ito, H., Sumrejkanchanakij, P., Adachi, S., Hiroe, M., Shimizu, M., Kawauchi, J., Sunamori, M., Marumo, F., Kitajima, S. et al. (2003). Critical role of cyclin D1 nuclear import in cardiomyocyte proliferation. *Circ. Res.* **92**, e12-e19.
- Tian, Y. C. and Phillips, A. O. (2002). Interaction between the transforming growth factor- $\beta$  type II receptor/Smad pathway and  $\beta$ -catenin during transforming growth factor- $\beta$ 1-mediated adherens junction disassembly. *Am. J. Pathol.* **160**, 1619-1628.
- Tremblay, K. D., Dunn, N. R. and Robertson, E. J. (2001). Mouse embryos lacking Smad1 signals display defects in extra-embryonic tissues and germ cell formation. *Development* **128**, 3609-3621.
- Trudel, M., Barisoni, L., Lanoix, J. and D'Agati, V. (1998). Polycystic kidney disease in SBM transgenic mice: role of c-myc in disease induction and progression. *Am. J. Pathol.* **152**, 219-229.
- Vainio, S. J. and Uusitalo, M. S. (2000). A road to kidney tubules via the Wnt pathway. *Pediatr. Nephrol.* **15**, 151-156.
- Winyard, P. J. D., Nauta, J., Lirenman, D. S., Hardman, P., Sams, V. R., Risdon, R. A. and Woolf, A. S. (1996). Deregulation of cell survival in cystic and dysplastic renal development. *Kidney Int.* **49**, 135-146.
- Yagi, K., Furuhashi, M., Aoki, H., Goto, D., Kuwano, H., Sugamura, K., Miyazono, K. and Kato, M. (2002). c-myc is a downstream target of the Smad pathway. *J. Biol. Chem.* **277**, 854-861.
- Yamaguchi, K., Shirakabe, K., Shibuya, H., Irie, K., Oishi, I., Ueno, N., Taniguchi, T., Nishida, E. and Matsumoto, K. (1995). Identification of a member of the MAPKKK family as a potential mediator of TGF- $\beta$  signal transduction. *Science* **270**, 1008-2011.
- Zhang, H. and Bradley, A. (1996). Mice deficient for BMP2 are nonviable and have defects in amnion/chorion and cardiac development. *Development* **122**, 2977-2986.